

RSC Advances



This is an *Accepted Manuscript*, which has been through the Royal Society of Chemistry peer review process and has been accepted for publication.

Accepted Manuscripts are published online shortly after acceptance, before technical editing, formatting and proof reading. Using this free service, authors can make their results available to the community, in citable form, before we publish the edited article. This *Accepted Manuscript* will be replaced by the edited, formatted and paginated article as soon as this is available.

You can find more information about *Accepted Manuscripts* in the [Information for Authors](#).

Please note that technical editing may introduce minor changes to the text and/or graphics, which may alter content. The journal's standard [Terms & Conditions](#) and the [Ethical guidelines](#) still apply. In no event shall the Royal Society of Chemistry be held responsible for any errors or omissions in this *Accepted Manuscript* or any consequences arising from the use of any information it contains.

Tyrosine-rich peptide induced flower-like palladium nanostructure and its catalytic activity

Received 00th January 20xx,
Accepted 00th January 20xx

DOI: 10.1039/x0xx00000x

www.rsc.org/

Young-O Kim,^{‡a} Hyung-Seok Jang,^{‡a} Yo-han Kim,^a Jae Myoung You,^a Yong-Sun Park,^b Kyoungsuk Jin,^b Onyu Kang,^c Ki Tae Nam,^b Jung Won Kim,^{*c} Sang-Myung Lee^{*d} and Yoon-Sik Lee^{*a}

A specifically designed peptide, Tyr-Tyr-Ala-His-Ala-Tyr-Tyr (YYAHAYY), induced the formation of flower-like palladium (Pd) nanostructure by controlling the size and shape of nanoparticles (NPs). The flower-shaped Pd NPs showed excellent catalytic activities in copper-free Sonogashira cross-coupling reaction in water.

Nature determines protein structures by arranging amino acid sequences through genetic controls. The protein tertiary structures can control the exquisite sizes and morphologies of inorganic hybrid structures with high reproducibility under physiological conditions.¹ For example, homogeneous iron oxide nanoparticles (NPs) (about 8–9 nm) are formed inside hollow polypeptide ferritin shells.² We speculated that not only the self-assembly of peptides but also the interaction between the peptides and metal ions is a key factor in fabricating organic-inorganic hybrid nanostructures. By mimicking this biological process, various metal (Au,^{3–5} Ag,^{6–8} Pd,^{9–11} Pt^{12–14} and Cu^{15,16}) NPs have been developed by using peptide templates with controllable geometrical, physical and chemical parameters. However, understanding the design rule for peptide sequences still remains a challenge.

We designed a heptapeptide, Tyr-Tyr-Ala-His-Ala-Tyr-Tyr (YYAHAYY) (Tyr-H7mer), to synthesize Pd NPs under ambient conditions. In our previous study,¹⁷ we reported that Tyr-containing peptides could be assembled into several nanostructures and at least two consecutive Tyrs were necessary for the peptide assembly. The Tyr also has a potential as a bio-catalyst due to its redox active property.¹⁸ To

control the size and stability of Pd NPs, His was inserted at the center of the peptide sequence. His can coordinate with several transition metal ions and nucleate the formation of metal NPs.¹⁹ We inserted His between the two Tyrs to control the size of Pd NPs by the peptide folding. As it turned out, Pd NPs (4–5 nm size) with flower shapes can be synthesized by Tyr-H7mer in water.

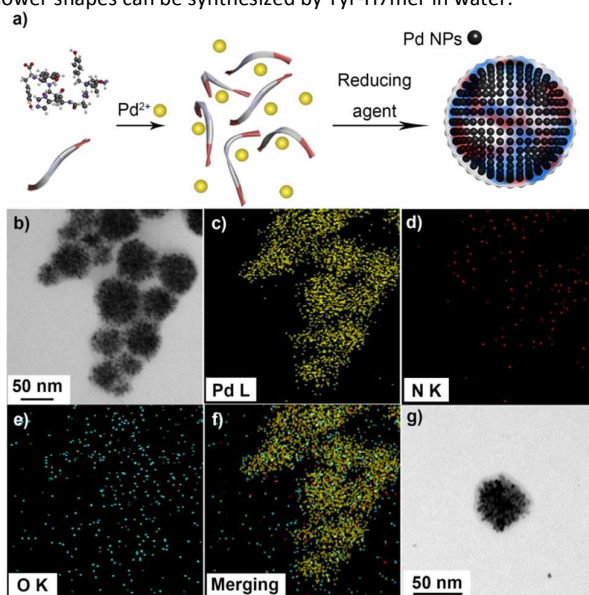


Fig. 1 (a) Schematic illustration of the formation of Pd nanoflowers covered by peptides. (b–f) HR-TEM/EDS mapping images of Pd NFs. The homogeneous distributions of palladium (c), nitrogen (d), oxygen (e) and merged one (f). (g) TEM images of Pd nanoflowers obtained by using the Tyr-H7mer as a template without reducing agent.

Among numerous metals, Pd has attracted much interest as an excellent catalyst for C–C cross coupling reactions, which are key reactions to produce fine chemicals such as dyes, pharmaceutical and agricultural intermediates, and so on.²⁰ The Pd catalysts can be used in the form of Pd²⁺ coordinated with ligands or metallic Pd⁰. Regarding Pd NP catalysts in particular, it is essential to precisely control the surface morphology of Pd nanostructures to improve

^a School of Chemical and Biological Engineering, Seoul National University, Seoul 151-744, Republic of Korea. Fax: +82-2-876-9625; Tel: +82-2-880-7073; E-mail: yslee@snu.ac.kr.

^b Department of Materials Science and Engineering, Seoul National University, Seoul 151-744, Republic of Korea. Fax: +82-2-883-8197; Tel: +82-2-880-7094; E-mail: nkitae@snu.ac.kr.

^c Department of Chemical Engineering, Kangwon National University, Samcheok 245-711, Republic of Korea. Tel: +82-33-570-6543; E-mail: jwemye@kangwon.ac.kr

^d Department of Chemical Engineering, Kangwon National University, Chuncheon 200-701, Republic of Korea. Fax: +82-33-251-3658; Tel: +82-33-250-6335; E-mail: sangmyung@kangwon.ac.kr

[†] Electronic Supplementary Information (ESI) available: Experimental details, supplementary figures. See DOI: 10.1039/x0xx00000x

[‡] These authors contributed equally to this work.

the catalytic activity.²¹ Here, we apply a biomimetic synthesis of Pd NPs using a newly designed peptide template. The resulting Pd NPs were used as eco-friendly heterogeneous catalysts for copper-free Sonogashira C-C cross coupling reactions. The catalytic reaction was performed in an aqueous medium and under mild conditions (65–75 °C) with high conversion.

Figure 1a illustrates the scheme for the formation of Pd nanoflowers with Tyr-H7mer. Pd²⁺ ions are coordinated with His residues of Tyr-H7mer in water, resulting in peptide folding. We found that the hydrophobic nature of the Tyr-H7mer/Pd²⁺ complex accelerated the peptide assembly and the Pd²⁺ ions were gradually reduced to Pd NPs. During the reduction process by ascorbic acid as a reducing agent, the color of the Tyr-H7mer/Pd solution turned from pale yellow to dark brown. The UV/Vis spectra also showed the absorption changes during the formation of Pd NPs by Tyr-H7mer in water (Figure S1 in Supporting Information). As shown in Fig. S1, the absorbance peak of Pd²⁺ at 207 nm gradually decreased and broadened during the formation of the Pd NPs.

Transmission electron microscopy (TEM) analysis revealed that uniform sized Pd NPs (4–5 nm) were assembled into flower-like shapes with our heptapeptides (Figure 1b). The EDS elemental mapping showed the distributions of Pd, N and O on the surface of Pd nanoflowers (NFs) (Figure 1c–f). Interestingly, the final morphologies of Pd NPs seemed to be dependent on the central amino acid in our peptide sequence. When His was substituted with Ala to produce YAAAYY (Tyr-A7mer), irregular shaped Pd nanoaggregates were formed (Figure S2). His could play an important role in peptide assembly with Pd²⁺ ions because the imidazole group of His can bind strongly with metal ions. Thus, the His residues of the peptides provided the nucleation sites for Pd NFs formation before nucleation and growth of Pd NPs.¹⁰ The sizes of Pd NFs were between 39 and 100 nm, with an average of 66 nm ± 5 nm (Figure S3). The Pd NPs could also be formed without adding any reducing agents. However, it took a very long time to form Pd NFs (4 weeks at room temperature) (Figure 1c). This seems to be related to the weak reducing activity of Tyr residues.²²

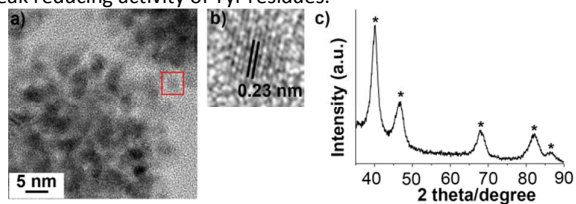


Fig. 2 (a) HR-TEM image of Pd nanoflowers. (b) HR-TEM image recorded from the particle (ca. 4 nm) marked by a red square in (a). (c) PXRD pattern of the Pd nanoflower. Pd peaks are indicated with a star (*).

The Pd NF was further characterized by high resolution transmission electron microscopy (HR-TEM) and powder X-ray diffraction (XRD) to identify the structure (Figure 2). The lattice structure of a single Pd particle in the Pd NF indicates the (111) plane of Pd (d-spacing at 0.23 nm) (Figure 2b and Figure S4). The Powder XRD pattern shows the crystallinity of Pd NFs. As shown in Figure 2c, peaks at 40.1°, 46.8°, 68°, 82.2°, and 86.4° correspond to the results indexed to the (111), (200), (220), (311), and (222) lattice planes of face-centered cubic (fcc) Pd.²³

The assembly mechanism for Tyr-H7mer during the formation of Pd NFs was identified by circular dichroism (CD) and Fourier transform-infrared (FT-IR) spectroscopy (Figure 3a). The richness of Tyr residues in our peptide sequence affected the entire pattern of the CD spectra.¹⁷ The positive peaks at 202 and 227 nm are originated from the contributions of the phenolic side chains of the Tyr residues. After adding Pd²⁺, the peak at 227 nm increased positively and was slightly red-shifted. The peak shifts of the Tyr residues indicate that Pd²⁺ ions are involved in peptide ordering.^{24, 25} The negative peak at 190 nm was reduced and shifted to 195 nm. It seems that the alpha helical conformation of Tyr-H7mer is affected by Pd²⁺ mediated peptide assembly. In addition, the amide I band region (Figure 3b, 1600–1700 cm⁻¹) was analysed to identify any conformational changes of the Tyr-H7mer during the assembly process.^{26, 27} As shown in Figure 3b, the alpha helical peak at 1670 cm⁻¹ was shifted to 1633 cm⁻¹, which corresponds to the beta sheet structure. After the reduction of Pd²⁺, the 1633 cm⁻¹ peak was shifted slightly to 1628 cm⁻¹.

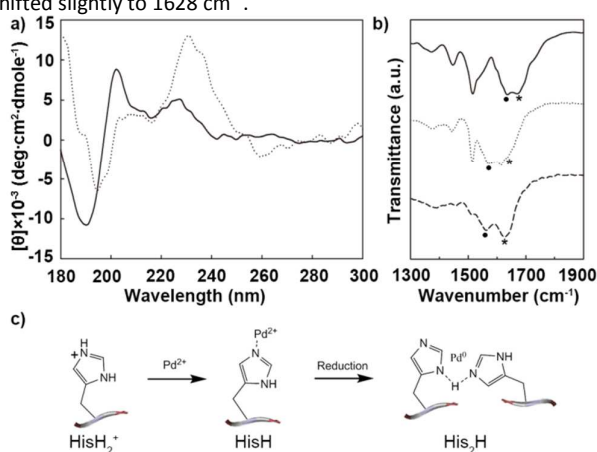


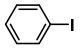
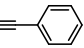
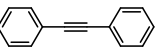
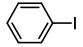
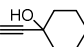
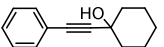
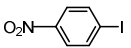
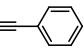
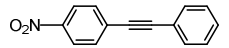
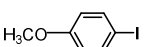
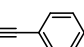
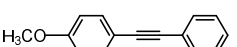
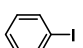
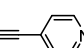
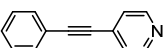
Fig. 3 a–b, Spectroscopic data for confirming peptide structural changes. Peptide, Pd²⁺/peptide complex, and reduced Pd NF produced by using peptide are indicated by line, dotted line, and dash line, respectively. (a) CD spectra of peptide changed by each step (b) The FTIR spectra of peptide changed by each step. Amide I band peaks are marked with star (*). Histidine-related peaks are marked with circle (•) (c) Proposed mechanism based on FTIR data focusing on interaction between Pd²⁺ and histidine residue in peptide

We could also confirm the interaction between the His residue and the Pd²⁺ ion by analysing FT-IR spectra of various protonated forms of the His side chain (imidazole group).²⁸ The His peak (HisH₂⁺) at 1635 cm⁻¹ of free Tyr-7Hmer in water was shifted to 1578 cm⁻¹ after the formation of Pd NFs, indicating the removal of one proton from HisH₂⁺. Afterward, the reduction of Pd²⁺ caused the peak to further shift to 1562 cm⁻¹. It may be possible that the His residue interacts with the closest His residue in the vicinity to produce dimers connected by hydrogen bonds. Considering all these, we believe that the Tyr-H7mer can act as a template for organizing the Pd²⁺ ions to form Pd NFs.

For atom efficiency and sustainability, a mild reaction condition for the Sonogashira cross-coupling reaction without using Cu(I) co-catalysts and phosphine ligands has been pursued. Fortunately, the Pd NFs have ideal properties as a catalyst for the Sonogashira cross-

coupling reaction under ambient aerobic conditions; accelerating oxidative addition of Pd⁰ with aryl halide by peptide ligand having steric and proper electronic property,²⁹ and enhancing the formation of arylalkynylpalladium species³⁰.

Table 1. Aqueous copper-free Sonogashira cross-coupling reaction using Pd NFs.^a

| Entry | Aryl halide | Alkyne | Product | Yield ^b (%) |
|-------|---|---|---|------------------------|
| 1 |  |  |  | 96 |
| 2 |  |  |  | 81 |
| 3 |  |  |  | 97 |
| 4 |  |  |  | 93 |
| 5 |  |  |  | 82 |

^a Reactions were performed using 0.5 mmol substrate, 2.5 eq. triethylamine, and 0.5 mol% Pd NFs in water (10 mL). ^b Determined by GC-MS through the corrected normalization of peak areas.

As shown in Table 1, a copper-free Sonogashira cross-coupling reaction catalyzed by Pd NFs was successfully performed in an aqueous condition. Coupling reactions of iodobenzene with two different alkynes (1-phenylacetylene and 1-ethyne-1-cyclohexanol) generated the corresponding products in 96 % and 81 % yields, respectively (entries 1 and 2). The catalyst was reused at least 4 times without structural collapse and significant loss of activity for the reaction with 1-phenylacetylene (Figure S5); the yields were over 91 % during the recycling. This catalytic system worked very well even though electron withdrawing substituents exist in the phenyl ring for the coupling reaction (entry 3). Three types of aryl iodides were reacted with phenylacetylene, producing the corresponding cross-coupling products in high yields over 93 % (entries 1 and 3, 4). Furthermore, the Pd NFs performed well in coupling reactions with heteroatom containing alkyne affording high yield (entry 5). Thus, we proved that the Sonogashira cross-coupling reaction was widely tolerable with various aryl iodides in the water system. These results are in good agreement with the previous report that stabilizer and supporting materials around Pd⁰ can prevent undesired aggregates and improved catalytic performance.³¹ In addition, the Glaser-type oxidative homocoupling side-reaction could be avoided due to not using copper salt.

In summary, we present a simple method for preparation of Pd nanostructure with a flower-like morphology using the Tyr-H7mer peptide template. The peptide folding and the interaction of Pd ions with His residues in the Tyr-H7mer are crucial for the nucleation and growth of Pd NPs to the Pd NFs. The Pd NFs are very reactive in copper-free Sonogashira cross-coupling reactions in an eco-friendly water solvent system. We demonstrate that controlling the morphology of metal NPs by redox active peptide is a novel method to fabricate a new type of metal-peptide hybrid catalysts.

Acknowledgement

This work was supported by Samsung Research Funding Center of Samsung Electronics under Project Number SRFC-MA1401-01.

Notes and references

1. S. Mann, *Nature*, 1993, **365**, 499-505.
2. B. R. Heywood, *Nature*, 1991, **349**.
3. C.-L. Chen, P. Zhang and N. L. Rosi, *J. Am. Chem. Soc.*, 2008, **130**, 13555-13557.
4. Y. Su, Q. He, X. Yan, J. Fei, Y. Cui and J. Li, *Chemistry-A European Journal*, 2011, **17**, 3370-3375.
5. T. Vinod, S. Zarzhitsky, A. Morag, L. Zeiri, Y. Levi-Kalisman, H. Rapoport and R. Jelinek, *Nanoscale*, 2013, **5**, 10487-10493.
6. D. Gottlieb, S. A. Morin, S. Jin and R. T. Raines, *J. Mater. Chem.*, 2008, **18**, 3865-3870.
7. C. J. Carter, C. J. Ackerson and D. L. Feldheim, *ACS nano*, 2010, **4**, 3883-3888.
8. M. Rubio-Martinez, J. Puigmartí-Luis, I. Imaz, P. S. Dittrich and D. Maspoch, *Small*, 2013, **9**, 4160-4167.
9. D. B. Pacardo, M. Sethi, S. E. Jones, R. R. Naik and M. R. Knecht, *ACS nano*, 2009, **3**, 1288-1296.
10. A. Jakhmola, R. Bhandari, D. B. Pacardo and M. R. Knecht, *J. Mater. Chem.*, 2010, **20**, 1522-1531.
11. R. Bhandari and M. R. Knecht, *ACS Catalysis*, 2011, **1**, 89-98.
12. C.-Y. Chiu, Y. Li, L. Ruan, X. Ye, C. B. Murray and Y. Huang, *Nature chemistry*, 2011, **3**, 393-399.
13. L. Ruan, H. Ramezani-Dakhel, C.-Y. Chiu, E. Zhu, Y. Li, H. Heinz and Y. Huang, *Nano Lett.*, 2013, **13**, 840-846.
14. L. Ruan, E. Zhu, Y. Chen, Z. Lin, X. Huang, X. Duan and Y. Huang, *Angew. Chem. Int. Ed.*, 2013, **52**, 12577-12581.
15. I. A. Banerjee, L. Yu and H. Matsui, *Proc. Natl. Acad. Sci. U.S.A.*, 2003, **100**, 14678-14682.
16. S. S. K. Dasa, Q. Jin, C.-T. Chen and L. Chen, *Langmuir*, 2012, **28**, 17372-17380.
17. H.-S. Jang, J.-H. Lee, Y.-S. Park, Y.-O. Kim, J. Park, T.-Y. Yang, K. Jin, J. Lee, S. Park and J. M. You, *Nat. Commun.*, 2014, **5**, 3665.
18. I. McConnell, G. Li and G. W. Brudvig, *Chem. Biol.*, 2010, **17**, 434-447.
19. R. Coppage, J. M. Slocik, B. D. Briggs, A. I. Frenkel, R. R. Naik and M. R. Knecht, *ACS Nano*, 2012, **6**, 1625-1636.
20. K. Nicolaou, P. G. Bulger and D. Sarlah, *Angew. Chem. Int. Ed.*, 2005, **44**, 4442-4489.
21. A. Mohanty, N. Garg and R. Jin, *Angew. Chem. Int. Ed.*, 2010, **49**, 4962-4966.
22. P. Selvakannan, A. Swami, D. Srisathiyarayanan, P. S. Shirude, R. Pasricha, A. B. Mandale and M. Sastry, *Langmuir*, 2004, **20**, 7825-7836.
23. T. Teranishi and M. Miyake, *Chem. Mater.*, 1998, **10**, 594-600.
24. A. K. Chen and R. W. Woody, *J. Am. Chem. Soc.*, 1971, **93**, 29-37.
25. R. W. Woody, *Biopolymers*, 1978, **17**, 1451-1467.
26. M. Jackson and H. H. Mantsch, *Crit. Rev. Biochem. Mol. Biol.*, 1995, **30**, 95-120.
27. P. Juszczak, A. S. Kołodziejczyk and Z. Grzonka, *J. Pept. Sci.*, 2009, **15**, 23-29.
28. A. Barth, *Prog. Biophys. Mol. Biol.*, 2000, **74**, 141-173.
29. N. S. Nandurkar and B. M. Bhanage, *Tetrahedron*, 2008, **64**, 3655-3660.
30. J. Cheng, Y. Sun, F. Wang, M. Guo, J.-H. Xu, Y. Pan and Z. Zhang, *J. Org. Chem.*, 2004, **69**, 5428-5432.

COMMUNICATION

ChemComm

31. R. Narayanan and M. A. El-Sayed, *J. Am. Chem. Soc.*, 2003, **125**, 8340-8347.

RSC Advances Accepted Manuscript